Towards a Topographic Microprocessor with TeraOPS Speed and Kilo Real-time Frame Rate

Tamás Roska[1,2], Csaba Rekeczky[2], Ákos Zarándy[1], András Radványi[1], István Szatmári[1], Tamás Szirányi[1,2], and Péter Szolgay[1]

[1]Analogical and Neural Computing Laboratory
Computer and Automation Research Institute
Hungarian Academy of Sciences
[2]Jedlik Laboratories, Péter Pázmány Catholic University
Phone: (+361) 2095263, Fax: (+361) 2095264, Email: roska@sztaki.hu

ABSTRACT

The analogic (analog and logic) cellular computer based on the CNN Universal Machine (CNN-UM) architecture is a new computing paradigm. It is a stored program ***topographic microprocessor****. Its CMOS mixed-signal implementation provides for a sensor array computer where the sensors are dynamically integrated with the processors. Hence, a content and context dependent sensor tuning can be implemented. Different sensormodalities including visual, auditory, tactile and other senses can be integrated and fused. Some practical applications, including robotics are outlined. The single chip implementations provide for TeraOps speed and Kilo real-time frame rate. The biological relevance is also discussed*

INTRODUCTION

Cellular Neural/Nonlinear Networks (CNN) [1]-[2] are locally connected massively parallel analog array processors. Completing the base cells with local memories, sensors, analog and logical arithmetics, and control units leads to the CNN Universal Machine (CNN-UM [3]), the architecture of a stored programmable visual microprocessor. Implementing this architecture on a single $1cm^2$ CMOS chip, an enormous computational power can be achieved reaching the order of TeraOPS (10^{12} equivalent digital operations per second). The computational capability makes it possible to solve a wide range of problems, including the discrete-space solution of 2D partial differential equations in microseconds and target detection and tracking with several 1k frames per second. The building of various stored programmable sensor-computers now in the horizon. The striking similarity to the anatomy of many living sensory systems makes the CNN-UM a must for bio-inspired computers and computing.

The application field of the CNN Technology is rich and also well developed. Many areas are covered in medical imaging (e.g. echocardiography analysis [11]), industrial quality control (e.g. texture segmentation [12], motion tracking [13]), etc.

THE CNN PARADIGM

A Cellular Neural/Nonlinear Network (CNN) is defined by two mathematical constructs [2]:

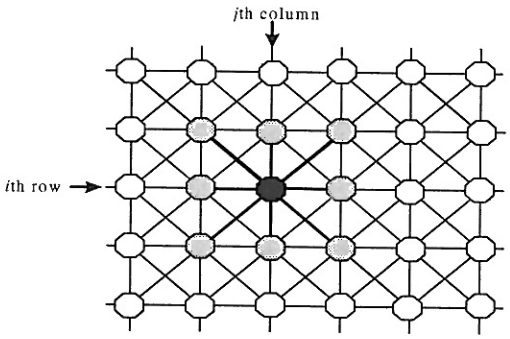

Figure 1 *A 2-dimensional CNN defined on a square grid.*

(i) A spatially discrete collection of continuous nonlinear dynamical systems called *cells*, where information can be encrypted into each cell via three independent variables called *input*, *threshold*, and *initial state*.

(ii) A local (synamptic) *coupling law* relating one or more relevant variables of each cell to all neighboring cells located within a prescribed sphere of influence $S_{r(ij)}$ of radius r centered at ij.

Fig. 1 shows a 2D rectangular CNN composed of cells that are connected to their nearest neighbors. Due to its symmetry, regular structure and simplicity this type of arrangement (a rectangular grid) is primarily considered in all implementations.

In a two dimensional (MxN) CNN array the cell dynamics is described by the following nonlinear ordinary differential equation:

$$C\frac{d}{dt}x_{ij}(t) = -R^{-1}x_{ij}(t) + \sum_{kl\in S_r} A_{ij,kl}\,y_{kl}(t) + \sum_{kl\in S_r} B_{ij,kl}\,u_{kl} + z_{ij}$$

$$y_{ij}(t) = f(x_{ij}(t)) = 0.5(|x_{ij}(t)+1| - |x_{ij}(t)-1|)$$

where x_{ij}, u_{ij}, y_{ij} are the state, input and output voltage of the specified CNN cell, respectively. The state and output vary in time, the input is static (time independent), ij refers to a grid point associated with a cell on the 2D grid, and $kl \in \Sigma_r$ is a grid point in the neighborhood within the radius r of the cell ij. Term $A_{ij,kl}$ represents the linear feedback, $B_{ij,kl}$ the linear control, while z_{ij} is the cell current (also referred to as bias or threshold) which could be space and time variant. The output characteristic f is a sigmoid-type piecewise-linear function.

CNNs with higher order base cells ("complex-cell" [5]) are also considered in latest architecture designs.

DIFFERENT CNN-UM IMPLEMENTATIONS

Typical implementation types are the digital CMOS (e.g. [17]), analog (mixed-signal) CMOS (e.g. [6]-[8]), and the optical (e.g. [9]). Although relying on digital CMOS implementation is the most straightforward from the design point of view, the performance of these digital chips falls far from the analog versions that can reach approximately TeraOPS: 10^{12} equivalent digital operations per second. It should also be noted that optical implementations are still in the experimental phase.

APPLICATIONS

The analogic cellular computer chips and systems are now available for a broad range of applications. We will show some of them, including medical imaging, multi spectral fusion, super high speed condition based maintenance, etc.

BIO-INSPIRED SENSORY COMPUTERS

The anatomy and physiology of many living sensory systems can be programmed on the CNN-UM. An outstanding example is the mammalian retina. These models and their combination with machine vision will be shown.

ACKNOWLEDGEMENTS

The partial support of the Hungarian Academy of Sciences and the Office of Naval Research is gratefully acknowledged.

REFERENCES

[1] L.O. Chua and L. Yang, "Cellular Neural Networks: Theory and Applications", *IEEE Transactions on Circuits and Systems*, Vol. 35, No. 10, pp. 1257-1290, October 1988.

[2] L.O. Chua and T. Roska, "The CNN Paradigm", *IEEE Transactions on Circuits and Systems - I*, Vol. 40, No. 3, pp. 147-156, March 1993.

[3] T. Roska and L.O. Chua, "The CNN Universal Machine: An Analogic Array Computer", *IEEE Transactions on Circuits and Systems - II*, vol. 40, pp. 163-173, March 1993.

[4] CNN BIBLIOGRAPHY: http://lab.analogic.sztaki.hu/ or http://www.ieee-cas.org/~cnnactc

[5] Cs. Rekeczky, T. Serrano-Gatarredona, T. Roska, and A. Rodríguez-Vázquez, "A Stored Program 2nd order/3-layer Complex Cell CNNM-UM", 6th IEEE International Workshop on Cellular Neural Networks and their Applications CNNA 2000, pp. 213-218, Catania, May 2000.

[6] S. Espejo, A.Rodriguez-Vázquez, R. A. Carmona, P. Földesy, Á. Zarándy, P. Szolgay, T. Szirányi, and T. Roska, "0.8μm CMOS Two Dimensional Programmable Mixed-Signal Focal-Plane Array Processor with On-Chip Binary Imaging and Instruction Storage", *IEEE Journal on Solid State Circuits*, Vol. 32. No. 7. pp.1013-1026, 1997.

[7] S. Espejo, R. Domínguez-Castro, G. Liñán, and Á. Rodríguez-Vázquez, "A 64x64 CNN universal chip with analog and digital I/O", 5th Int. Conf. Electronics, Circuits and Systems *(ICECS-98)*, Lisbon, pp. 203-206 1998.

[8] A. Paasio, A. Kananen and V. Porra, "A 176 x 144 processor binary I/O CNN-UM chip design", Eu. Conf. Circuit Theory and Design - *ECCTD'99 DAD*, Stresa, 1999

[9] Sz. Tőkés, L. Orzó, Cs.Rekeczky, T. Roska and Á. Zarándy, "An Optical CNN Implementation with Stored Programmability", IEEE International Symposium on Circuits and Systems ISCAS 2000, pp. 136-139, Geneva, June 2000.

[10] I. Szatmári, A. Schultz, Cs.Rekeczky, T. Kozek, T. Roska, and L. O. Chua, "Morphology and Autowave Metric on CNN Applied to Bubble-Debris Classification", *IEEE Trans. on Neural Networks*, Vol. 11, No. 6, pp.1385-1393, November 2000.

[11] Cs. Rekeczky, Á. Tahy, Z. Végh, and T. Roska, "CNN-based Spatio-temporal Nonlinear Filtering and Endocardial Boundary Detection in Echocardiography", International Journal of Circuit Theory and Applications, Vol. 27, pp. 171-207, 1999.

[12] T. Szirányi, M. Csapodi, "Texture Classification and Segmentation by Cellular Neural Network using Genetic Learning", *C. Vision and Image Understanding*, Vol. 71, No. 3, pp. 255-270, 1998.

[13] L. Czúni, T. Szirányi, "Motion Segmentation and Tracking with Edge Relaxation and Optimization using Fully Parallel Methods in the Cellular Nonlinear Network Architecture", *Real-Time Imaging*, (in press), 2001

[14] Cs. Rekeczky, "Locally Adaptive Image Processing Based on PDE and non-PDE related Diffusion Models", DNS-3-2001, Technical Report, Analogical and Neural Computing Laboratory, Computer and Automation Institute of the Hungarian Academy of Sciences, Budapest, February 2001.

[15] Cs. Rekeczky and L. O. Chua, "Computing with Front Propagation: Active Contour and Skeleton Models in Continuous-time CNN", Journal of VLSI Signal Processing Systems, Vol. 23, No. 2/3, pp. 373-402, November-December 1999.

[16] Á. Zarándy, F. Werblin, T. Roska, and L. O. Chua, "Spatial-logic Algorithms Using Basic Morphological Analogic CNN Operations", International Journal of Circuit Theory and Applications, Vol. 24, pp. 283-300, 1996.

[17] Á. Zarándy, P. Keresztes, T. Roska and P. Szolgay, "CASTLE: an Emulated Digital CNN Architecture: Design Issues, New Results", in Proc. 5th Int. Conf. on Electronics, Circuits and Systems (ICECS'98), pp.199-202, Lisbon, September 1998.

Advancement of MEMS & Nano Technology

Sukhan Lee; Byeungleul Lee; Jaejoon Choi; Jaewoo Chung; Hyunjung Shin ;Jong Up Jeon

Samsung Advanced Institute of Technology
P.O. Box 111, Suwon 440-600, Korea
Tel : +82-31-280-9008 ; Fax : +82-31-280-6565 ; E-mail : lsh@sait.samsung.co.kr

Abstract

This paper presents recent advancements of Si-based micro sensors and actuators at Samsung Advanced Institute of Technology (SAIT), including a high performance of micro gyroscope, an electrostatic micro actuator for HDD, and a piezoeletric actuator on silicon membrane for inkjet printing.

The micro gyroscope presented here shows recent progress in sensitivity and mass producibility based on structural decoupling, SOG-based fabrication, and wafer level vacuum packaging. To achieve the maxinum power to volume ratio, the eletrostatic micro actuator is designed with an optimal geometric layout of rotors and stators, that leads to more than 4 times of force/torque efficiency. We have been successful for the design and fabrication of a piezoeletric micro actuator on a silicon membrane that can be applied to inkjet printing.

Keyword : Micro Gyroscope, Micro Electrostatic Actuator, Piezoelectric Actuator, Silicon Machining, SOG process, SPM, Silicon Membrane.

I. Micro Gyroscope

Gyroscopic devices for measuring angular rate have been the subject of extensive research and development over the past several decades. There has been considerable interest in the development of a low-cost and small sized gyroscope, since many applications, such as a navigation apparatus for automobiles or a sensor for compensating the hand-quiver in video camera, etc., exist for the devices.

As representative micro inertial sensors, silicon based gyroscope is being considered as the next mass-product mechanical sensors after silicon pressure sensors. This section will focus on the recent advances that have been in R&D of silicon based vibratory micro-gyroscope.

Surface Micro-machined Gyroscope

Recently several works on micro mechanical gyroscope have been reported, and most of these sensors are vibratory type. This vibratory gyroscope is driven in a resonant state by electrostatic force and detected the output due to a capacitance change between the mass plate and the bottom electrode.

The Coriolis motion arising from the angular rate causes the capacitance change and is converted to voltage change. Figs. 1 and 2 shows the SEM photographs of the single axis and dual axis gyroscope[1][2] developed in SAIT, respectively.

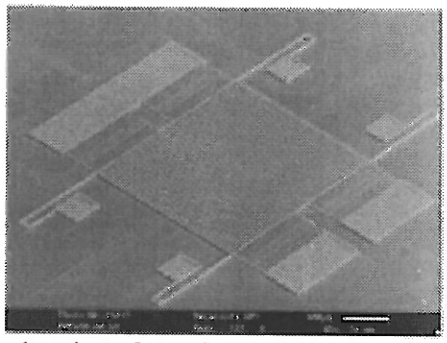

Fig. 1 Single axis surface micro-machined gyroscope

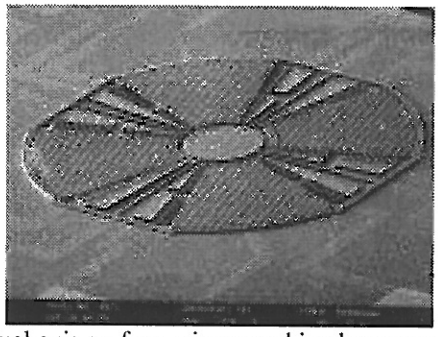

Fig. 2 Dual axis surface micro-machined gyroscope

These surface micro-machined gyroscopes were fabricated by using the thick poly-silicon processes, and vacuum packaged in individual level. The inside vacuum pressure and the quality factor were 50 mTorr and above 1000, respectively. Figure 3 shows the case vacuum packaging results. These sensors showed a noise equivalent rate of 0.1deg/sec, and sensing rage of 100 deg/sec.

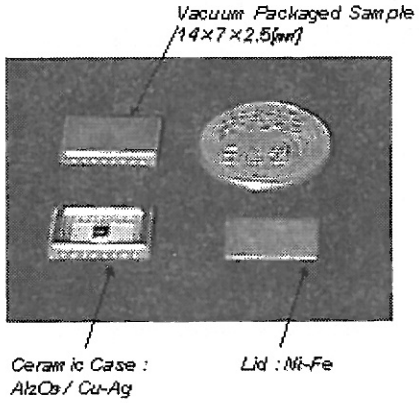

Fig. 3 Vacuum packaged sample

Bulk Micro-machined Gyroscope

The surface micro-machining using LPCVD poly-silicon is one of the most convenient process as for MEMS. However, the LPCVD poly-silicon layer easily gets residual stress and stress gradient that make micro-structure unstable. Furthermore, for the high sensitive design, the thick structure is needed, but it is hard to fabricate over 10□-thick LPCVD poly-silicon structure.

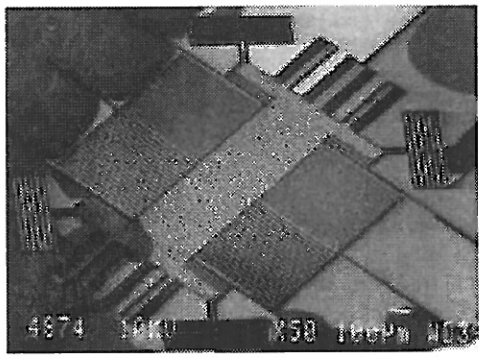

Fig. 4 SOG processed gyroscope

Figure 4 shows the SEM photograph of the SOG(silicon on glass) processed gyroscope.[3] It is very simple to fabricate the gyroscope with a total chip size of 3×3.5×1□ using only one mask. The gyroscope structure is fabricated on an anodic bonded 40um-thick silicon on glass. After the top silicon is etched using a deep RIE, a part of the glass under the silicon structure is etched by HF for releasing the top silicon structure. Since the depth of the etched glass under the silicon structure is about 20~30mm, the damping and the stiction between the structure and the glass substrate are minimized. The minimum gap and the aspect ratio of this structure is 2mm and 20, respectively. Without an additional frequency tuning method, it is demonstrated that the difference between the two frequencies is about 85Hz, and the noise equivalent rate is 0.05deg/sec at 50mTorr pressure.

Mixed Micro-machined Gyroscope

In the resonant vibratory gyroscope, when the driving and sensing frequencies are exactly tuned, the sensitivity is maximazed. However the coupled gyroscope that used same springs in driving and sensing mode shows mode coupling effect. Therefore, the coupled gyroscope is barely matched, even though the device has electrostatic tuning capability. Figure 5 shows the schematic drawing of the decoupled vertical gyroscope.

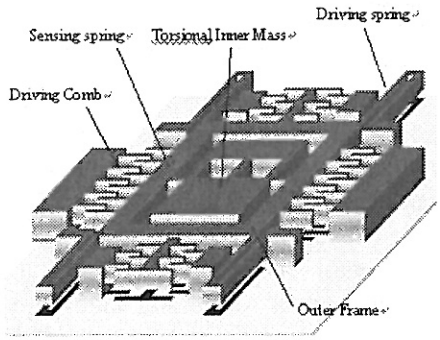

Fig. 5 De-coupled vertical gyroscope

The mixed micro-machining process has merits of the surface and bulk fabrication processes.[4] The single crystal silicon structure with a high aspect ratio can be fabricated without residual stress or stress gradient. Furthmore, it can fabricate the structure as various as the surface micro-machining process.

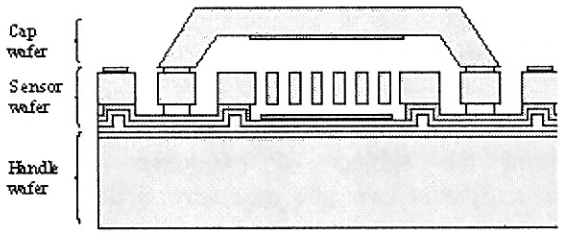

Fig. 6 Cross view of mixed-processed gyroscope

Figure 6 shows the cross sectional view of the mixed micro-machined gyroscope. The device has 3 level stack structures of silicon wafer. The vibrating structures are made of 40□ thick polished sensor wafer layer.

The vacuum environment for operating a vibratory gyroscope was accomplished with wafer level vacuum packaging using the cap wafer in fig.6. The vacuum level of ambient pressure was

about 150mTorr. Figure 5 shows the SEM photograph of the wafer level vacuum packaged gyroscope.

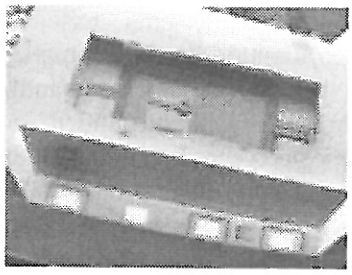

Fig. 7 Vacuum packaged SAIT gyroscope

The resolution of the gyroscope was 0.013deg/sec/√Hz, and the output nonlinearity was below 2% in ±100deg/sec FS.

II. Optimally shaped secondary micro-actuator for HDD

By the current annual increasing rate of 60%, data recording densities are expected to reach 10 Gb/in2 by 2001 year. To achieve recording density of 10 Gb/in2, data track density has to be reached to 25000 TPI. Therefore accurate and fast positioning technique of read/write head element is needed and a development of dual stage actuator using MEMS is also needed.

Fig.1 shows a concept of dual-stage system. A VCM is used as coarse track position actuator and micro-actuator, is located between slider and suspension, is used as fine position actuator.

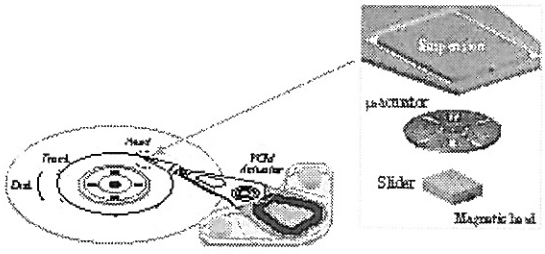

Fig. 1. A concept of dual stage servo system

Actuator Design

Electrostatically driven micro actuator with optimally designed electrodes for the large excitation force was developed

Fig.2 (a) shows the curved shaped parallel electrodes that was designed in SAMSUNG and (b) shows the electrode that was designed at IBM and U.C. Berkeley [1,2]. (c), (d) shows the simulated results for the excitation force for each design. At the condition of the same size and gap between the two parallel electrodes, curved shaped electrodes has a larger excitation force about 4.6 times compared to the IBM type. Because of the large excitation force of curved shaped electrodes, the frequency characteristics of micro actuator can be improved.

We also developed the micro actuator that has a saw-tooth shaped electrode in Fig.3. Because of this shape, the stiffness of the rotor electrode can be also increased

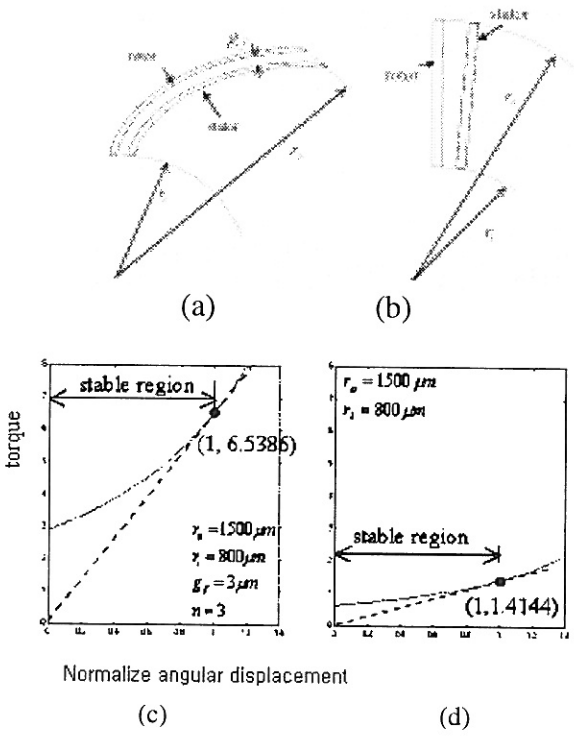

Fig. 2. A comparision of micro actuator design
(a, c: SAIT / b, d : IBM, U.C. Berkerly)

Structure of Micro-Actuator

As shown is Fig.3, the actuator consists of stator wirh fixed outer ring, rotor with a mobile inner ring. A inner ring is meshed for minimizing rotor's moment of inertia.

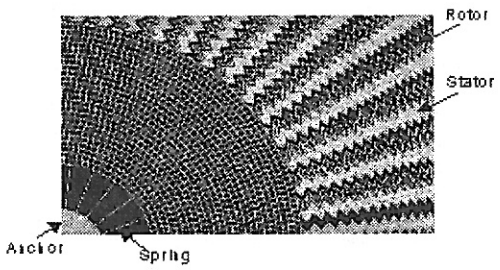

Fig. 3. A quarter view of saw shape micro-actuator

Fabrication Process

Fig.4 shows the fabrication process that use SOG(Silicon on Glass) wafer.

First, Si was bonded to the Pyrex glass and polished to the desired thickness. Second, metal was sputtered and patterned. Third, Si is etched through by ICPRIE and finally glass was etched by HF for the releasing of the structure.

By this SOG process, microactuator that has a high aspect ratio over 1:15 easily with low cost.

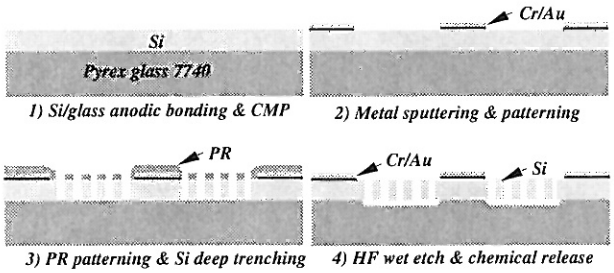

Fig. 4. A fabrication flow chart of micro-actuator using SOG(Silicon on glass) process

Results

Microactuator whose diameter is 3.4 mm, is shown in Fig.5. The 3□ capacitive gap between electrodes has a maximum aspect ratio of 15:1. a angular displacement of micro actuator is about ±1um, resonant frequency is 3.6 KHz at DC 8V, AC 7V. This results fit well with the simulated one.

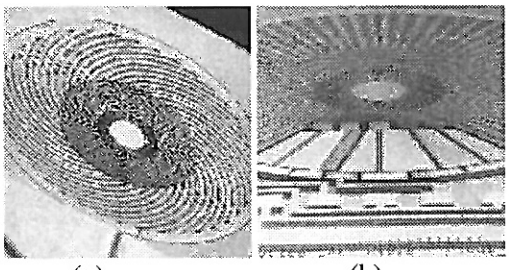

(a) (b)

Fig. 5. SEM photographs of electrostatic type secondary micro-actuator (a: curved shape, b: saw shape)

III. Ultra-high Information Density Storage System based on Scanning Probe Microscopy

Since IBM introduced the first disk drive in 1957, the data storage systems based on magnetic recording technology has had remarkable advances. Currently the area density of manufactured HDD reaches almost 14 Gbits/in^2 and is increased at the rate of 60% per year. In 1990, for example, HDD had an areal density of less than 0.1 Gbits/in^2. This technological limitation will not stop the need for greater storage capacity in less space. However, it is believed that the current magnetic recording technology used in HDD has a critical limit – super-paramagnetic limit - that is due to the thermal energy causing the de-magnetization of the information bits with smaller size. The next generation data storage systems need much higher density, at least greater than 100 Gbits/in^2, beyond the incremental advance of an existing technology. Therefore, new read and write technology in nano-meter scale is required to investigate.

An information storage system utilizing scanning probe microscope (SPM) technique could be the most feasible one to perform nano-scaled recording.[7] This is simply because the storage devices using SPM can be achieved higher information storage density than any other methods being investigated currently. Many researchers have proposed various SPM based storage techniques such as scanning tunneling microscope (STM), atomic force microscope (AFM), magnetic force microscope (MFM), and scanning near-field optical microscope (SNOM), as future ultra-high density data storage systems. Most of the works are addressing the fundamental understanding of the mechanisms and interactions between the tip and sample. In the case of AFM-based storage, works toward storage devices in our research group as well as others[8] have progressed beyond simply demonstrating the ability to make a small information bit.

Most of the AFM-based storage, to store information with spatial resolution in tens of nanometer or below, demonstrates successfully write-once read-many (WORM) type storage. In particular, piezoresponse of ferroelectric thin films provides a unique way to read/write of information bits many times in the AFM-based storage system. Applying dc pulses through a conductive tip, domains of nanometer size can be purposely formed in two opposite directions. This domain can be labeled either "0" or "1" depending on its polarization direction, thereby acting as a bit in a

memory device.

To investigate the feasibility of utilizing PZT films as data storage media, the formation of a series of data dots was demonstrated and its result is shown in Fig. 1. Initially a 10 μm × 10 μm area was scanned with the tip biased to -15 V. In a "write operation" the tip was travelling along the desired traces with a 100 μs pulse and a voltage of +14 V. The scanning speed was 1 μm/sec. The formed bits were in the size of 60-100 nm in diameter with bright contrast, implying high information density (larger than 100 Gbits/in^2).

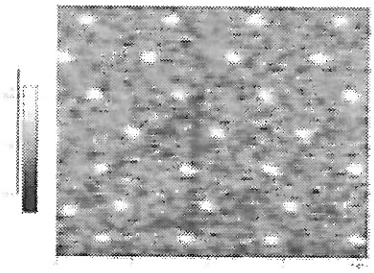

Fig.1 An piezoresponse image of induced ferroelectric domains as information dots polarized with a +14V, 100 ms, which shows a potential application of mass storage system

Ferroelectric domains in nano-meter scale were formed by applying voltages of –27.0, –21.6, –18.0, –16.2, –14.4, –10.8, and –7.2 V to the bottom electrode while the tip was grounded. No ferroelectric domains were found with the applied voltage of –6.5 V or below. Pulse width was 33 ms and scan speed was 2.5 μm/sec. The film thickness was 270 nm. Fig. 2 shows the bit size variation as a function of applied voltage. The size of the bits was obtained from the amplitude and phase images of the first harmonic signal. It is clear that the size of the bits is linearly dependent upon the applied voltage. Inhomogeneity of the electric field between the AFM tip, which has small radius of curvature (<10 nm), and infinite bottom electrode leads to larger bits formed upon higher voltage applied.

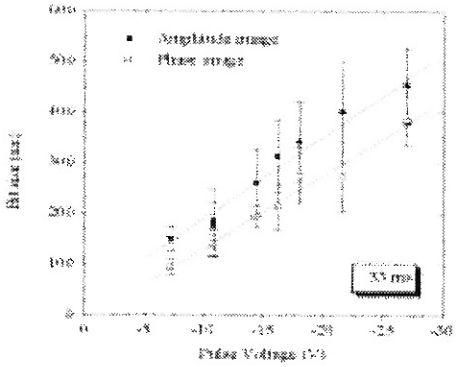

Fig. 2 shows the bit size variation as a function of applied voltage

IV. A Drop on Demanded Piezo Inkjet Printhead

The demand for higher image quality inkjet printhead has intensified along with the explosion in recent years of color digital images. Various types of ink jet printheads have been produced and supplied to a variety of market. [1] For the generation of an inkjet there is a variety of actuation principles, such as shear. push and bending modes, each of which has gained its market share. We have been developing piezo inkjet head by bending mode technology. Using computer modeling, many variations of inkjet can be designed and tested. Our inkjet head comprised two major parts that are piezo actuator and flow channel prepared by micro machined Si crystals. SAIT encountered several technological challenges during the development of the inkjet head for high performance. Several types of inkjet proto heads prepared with different kind of nozzle density (cpi) provided us successive in drop ejection. Among them, the fabrication and their evaluations inkjet heads developed are shown in this architecture.

Ink jet Head

Ink jet head design is a complex and iterative process that attempts to satisfy many constants[2]. The schematic of a cross-section inkjet head is shown in Fig. 1.

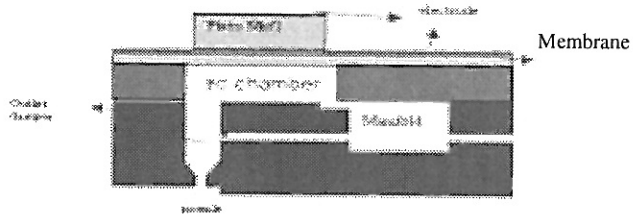

Fig. 1 ; Schematic of piezo inkjet head

The flow channel composes five parts such as, pressure chamber, manifold, outlet damper, restrictor and nozzle. Each pressure chamber is divided by upper plate. It provides the separation walls necessary to prevent crosstalk effects. The manifold supplies ink into the pressure chamber. The outlet damper plays a role to avoid inclined fluidic flow as well as keeping straight drop ejection out of nozzle. The ink can be prevented from reverse flow into manifold when the chamber is pressurized by piezo actuator. A piezo electric element is changing the volume of an ink chamber inducing drop ejection through the nozzles. The nozzle is intimately related to the speed of ink drop changing the size of its diameter. Piezo actuators are fabricated as thick film of 20 □m on Si

diaphragm forming the bimorph structure. The expansion and contraction of the piezo materials fires ink droplets. To be able to determine the ratio of piezo material to diaphragm, we adopted the modeling using the equations[3] as follow ;

$$\delta = \frac{3l^2 d_{31} E.g(m,n)}{T_p} = \frac{3l^2 d_{31} E}{T_s} \cdot \frac{g(m,n)}{n} \quad (1)$$

$$g(m,n) = \frac{mn^2(n+1)}{m^2 n^4 + 4mn^3 + 4mn + 1} \quad (2)$$

where,

l ; length of cantilever, E ; electric field, Tp ; Thickness of piezo material

Ts ; thickness of elastic diaphragm, m ; Y's Modulus ratio between piezo material and diaphragm, n ; thickness ratio between piezo material and diaphragm

The function of g(m,n) give us the plot as Fig. 2, From this relation, it is certain that the deflection is dependent on the size and physical properties.

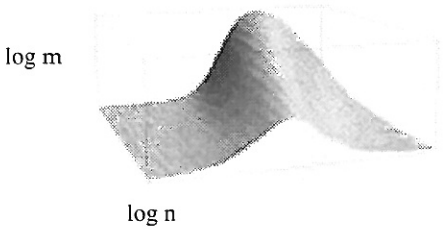

Fig. 2 ; g (m, n)

In a case of diaphragm thickness fixed, it's thickness can be determined considering the stress of elastic diaphragm, the stability of controlled thickness, and force necessary for actuator. The deflection should be changed according to the thickness of piezo materials. Fig. 3. The maximum deflection was obtained at the thickness ratio about 1.25 keeping the diaphragm 20 um, width of the piezo device relative to the ink chamber. However, upon considering the displacement and displacement x pressure, which determine the volume and speed of ink droplet ejection, [4], we adopted 10 um diaphragm for the 20 um piezo device.

Inkjet heads were fabricated and observed by specific input pulse shape. The result is shown in Fig. 4.

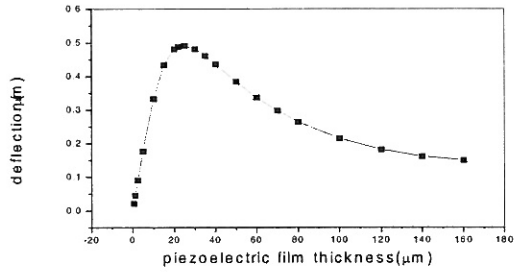

Fig. 3 : Deflection change in relation to thickness of piezo material at fixed thickness of diaphragm

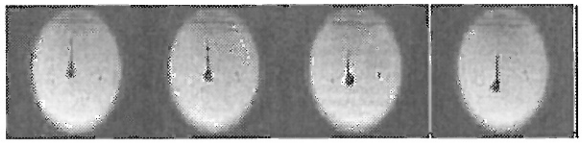

Fig. 4 ; Drop ejection

Each of drop velocity and volume was measured 3~5 m/sec, about 15 pl, respectively. The fire frequency ranges from 1 kHz to 12 kHz.

Higher resolution necessitates scaling jet designs to decrease drop volumes, while maintaining the high drop velocities needed for accurate drop displacement. To obtain higher performances, we are under development of the inkjet head with continuity to change many constants and control the process parameters.

Conclusion

This paper illustrates the effectiveness of using SOG and decoupled structure for designing high sensitivity of micro gyroscopes. Shown also is the dramatic improvement of the force capability of electrostatic micro actuators by a proper layout of rotor-stator combinations. A method of designing and fabricating a piezoelectric micro actuators on a filmed membrane is provided.

References

1. B. Lee et al., "A dynamically tuned vibratory micro-mechanical gyroscope-accelerometer", Proceeding of SPIE(Smart electronics and MEMS), Adelaide, Australia, 1997
2. S. An et al., "Force-balanced dual-axis microgyroscope", Proceeding of SPIE(Smart electronics and MEMS), Adelaide, Australia, 1997
3. S. Baek et al., "A symmetrical z-axis gyroscope with a high aspect ratio using simple and new process", MEMS 1999

4. H. Song et al., " A wafer level vacuum packaged de-coupled vertical gyroscope by a new fabrication process", MEMS 2000, Miyagi , Japan, Jan. 2000.
5. David A. Horley, Albert P.Pisano, "Design and fabrication of an angular microactuator for magnetic disk drives", journal of microelectromechanical systems, Vol.7, No.2, 1998, pp.141~148
6. Long-Sheng Fan, Toshiki Hirano, "Electrostatic microactuator and design consideration for HDD application", IEEE transaction on magnetics, Vol.35, No.2, 1999, pp.1000~1005
7. H.J. Mamin, B.D. Terris, L.S. Fan, S. Hoen, R.C. Barrett, and D. Rugar, "High-density Data Storage using Proximal Probe techniques", *IBM J. Res. Develop.* **39**(6), 681-700 (1995)
8. M. Despont, J. Brugger, U. Drescher, U. Durig, W.Haberle, M. Lutwyche, H. Roithuisen, R. Widmer, H. Rohrer, G.K. Binnig, and P. Vettiger, in *IEEE Int. Micro Electro Mechanical Systems Tech. Dig.*, 564 (1999)
9. Hue P. Le, "Progress and Trends in ink jet printing Technology", Journal of Imaging Science and Technology, Vol. 42, 1, Jan./Feb., p49~62 (1998)
10. Ronald F. Burr, David A. Tence, and Sharon S. Berger, " Multiple Dot size Fluidics for phase change Piezoelectric Ink jets", Recent Progress in Ink jet Technologies II, edited by Eric Hanson, Society for Imaging Science and Technology, chap. 3, p192~198 (1999)
11. M. R. Steel, F. Harrison, and P. G. Harper, " The piezoelectric bimorph ; An experimental and theoretical study of its quasistatic response", J. Phys. D., vol. 11, p979~989 (1978)
12. Minoru Usui, " Development of the new MACH, "Recent Progress in Ink jet Technologies II, edited by Eric Hanson, Society for Imaging Science and Technology, chap. 3, p199~202 (1999)